nature astronomy

SUPPLEMENTARY INFORMATION

https://doi.org/10.1038/s41550-017-0288-9

In the format provided by the authors and unedited.

# The shock-heated atmosphere of an asymptotic giant branch star resolved by ALMA

**Wouter Vlemmings[1]*, Theo Khouri[1], Eamon O'Gorman[2], Elvire De Beck[1], Elizabeth Humphreys[3], Boy Lankhaar[1], Matthias Maercker[1], Hans Olofsson[1], Sofia Ramstedt[4], Daniel Tafoya[1] and Aki Takigawa[5]**

[1]Department of Space, Earth and Environment, Chalmers University of Technology, Onsala Space Observatory, 439 92 Onsala, Sweden. [2]Dublin Institute for Advanced Studies, 31 Fitzwilliam Place, Dublin 2, Ireland. [3]ESO Karl-Schwarzschild-Strasse 2, 85748 Garching, Germany. [4]Department of Physics and Astronomy, Uppsala University, Box 516, 751 20 Uppsala, Sweden. [5]The Hakubi Center for Advanced Research/Division of Earth and Planetary Sciences, Graduate School of Science, Kyoto University, Kitashirakawa-Oiwakecho, Sakyo, Kyoto 606-8502, Japan. *e-mail: wouter.vlemmings@chalmers.se

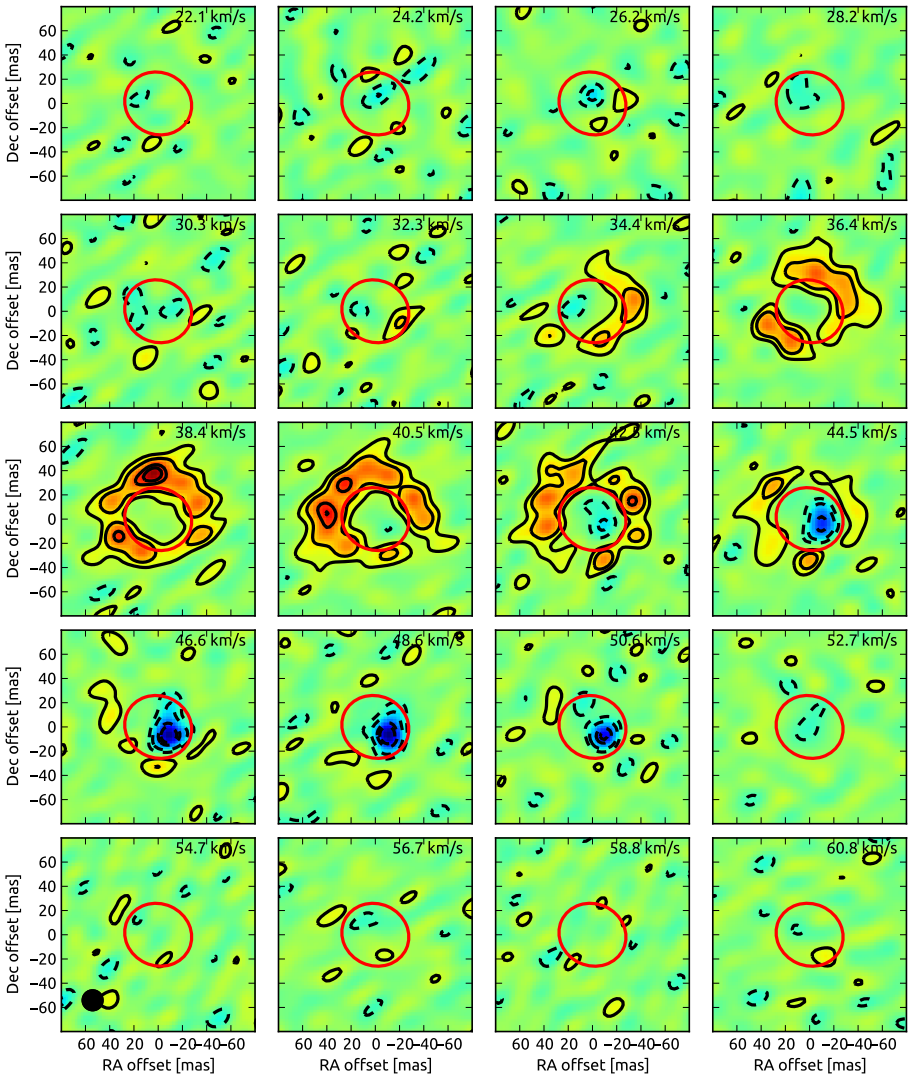


***Supplementary Figure 1.*** *Channel maps of the vibrationally excited pure-rotational transition of CO J=3-2, v=1 at 342.646 GHz around W Hya. As in Fig.1, the images were made using uniform weighting and restored with a circular 17 mas beam. Contours are drawn at -8, -6, -4, -2, 2, 4, 6, and 8 times the rms channel noise, which is 2.6 mJy Beam$^{-1}$. The velocity resolution for these images was reduced to ~2 km s$^{-1}$. The ellipse in each panel indicates the stellar disk at 338 GHz. The maps are dominated by red-shifted absorption, and the emission peaks around the stellar velocity, determined to be $V_{*,lsr}$ = 39.2 km s$^{-1}$.*

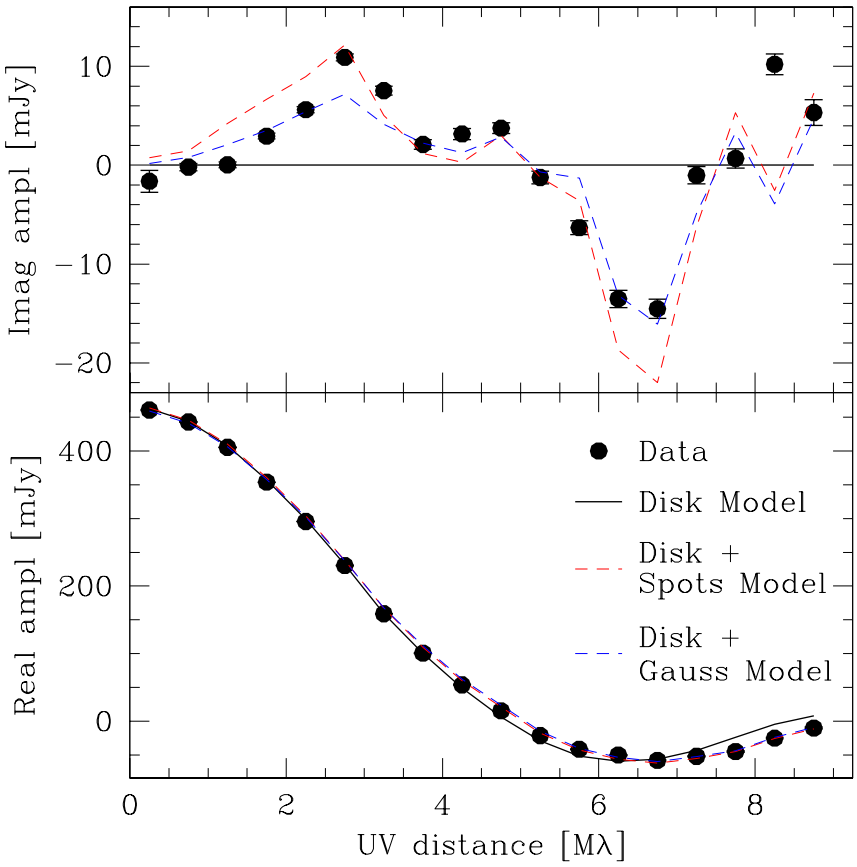


***Supplementary Figure 2***. *Azimuthally averaged Real (bottom) and Imaginary (top) amplitudes of the source visibilities against baseline length. In blue, we include the model of a disk with a single Gaussian component that is consistent with a point source. In red, we also include the best-fit disk model with 4 additional compact components. The parameters for both models are described in the text. The residuals of the disk + single component fit are shown in Supplementary Figure 3, and the residuals of the disk + multiple component fit are shown in Supplementary Figure 4. The error bars on the data points are indicated and in most cases are smaller than the symbol size. The deviations from a uniform disk are obvious both at long baselines in the Real amplitudes and in particular in the Imaginary amplitudes. As indicated by the fit including the compact spots, the imaginary amplitudes show a pattern consistent with off-center hotspots across much of the baseline range. Specifically the residual maps in Supplementary Figures 3 and 4 show the improvements when including more than a single component.*

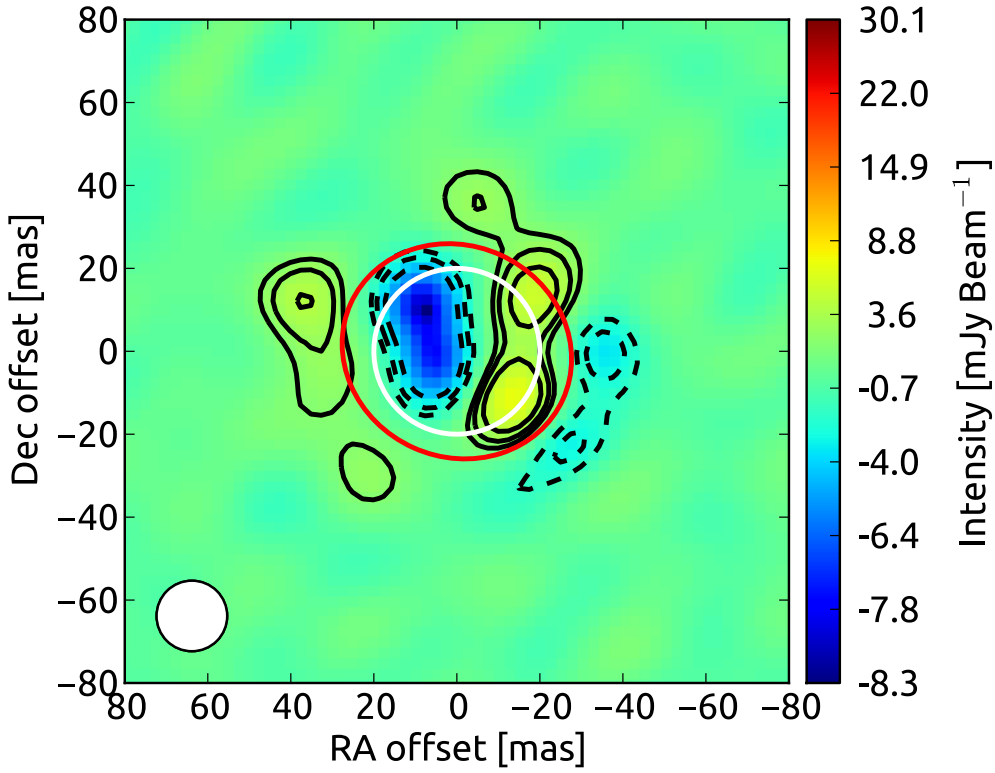


***Supplementary Figure 3.*** *The residual map after subtracting a uniform elliptical disk and a single Gaussian component from the continuum image of W Hya at 338 GHz. The size of the Gaussian component is fit to be* $0.1^{+0.4}_{-0.1}$ *mas and is thus consistent with an unresolved component. Contours are drawn at -9, -6, -4, 4, 6, 9 and 12 times the image rms noise of 0.45 mJy Beam*$^{-1}$*. Compared to Fig.2 of the main text, the residuals have decreased. Significant (>6*$\sigma$*) deviations from a uniform disk are still visible.*

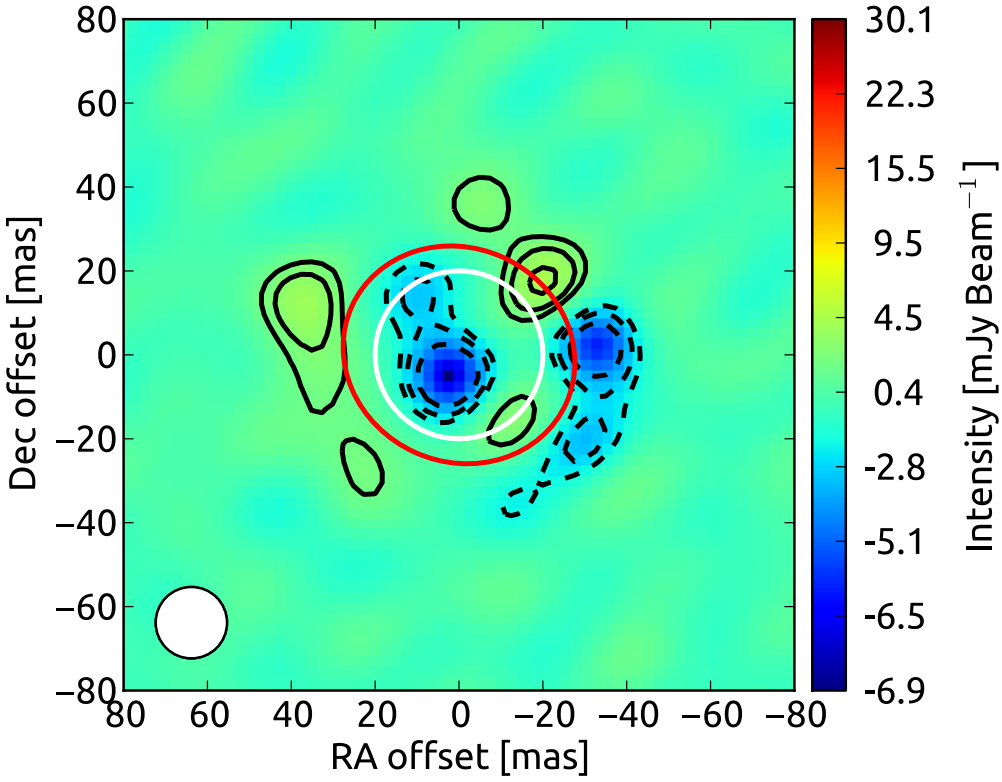


***Supplementary Figure 4.*** *The residual map after subtracting a uniform elliptical disk and four compact components from the continuum image of W Hya at 338 GHz. Contours are drawn at -9, -6, -4, 4, 6, 9 and 12 times the image rms noise of 0.45 mJy Beam$^{-1}$. Compared to Supplementary Figure 3, the residuals have decreased by 30%, highlighting the existence of more than one component. However, further deviations from a uniform disk are still obvious.*

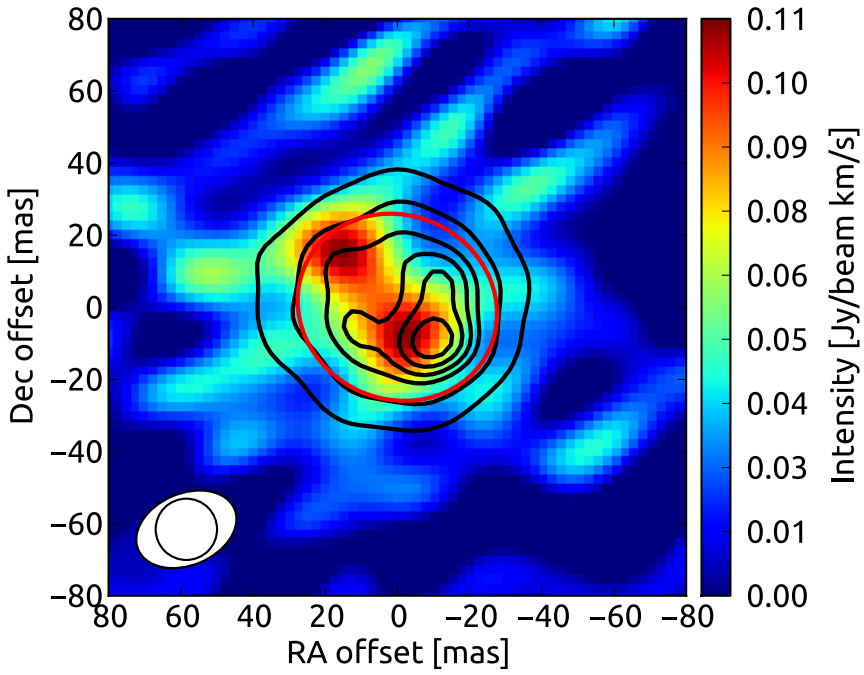


***Supplementary Figure 5***. *The background image is the integrated intensity of the unidentified line that is seen in emission against the warm stellar continuum (shown in black contours). The red ellipse indicates our fit to the stellar disk. The line is tentatively identified as the rotational transition* $J_{Ka,Kc} = 27_{3,25} - 28_{0,28}$ *in the vibrationally excited* $SO_2(v_2=2)$ *bending mode. It appears to originate from the hot molecular gas layer. The dirty beam size and the adopted restoring beam are shown in the bottom left.*

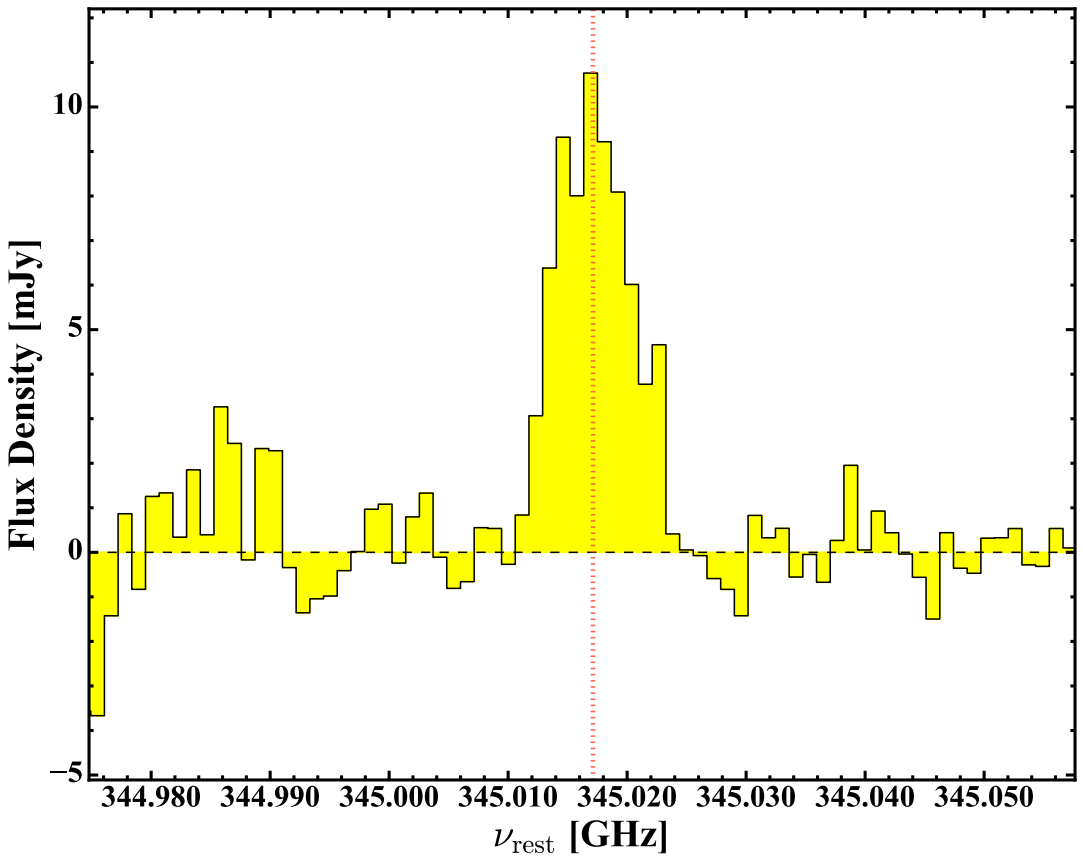


***Supplementary Figure 6***. *The rest frame spectrum of the unidentified emission line extracted against the stellar continuum. The spectrum is corrected for a stellar velocity of* $V_{*,lsr}$ *= 39.2 km* $s^{-1}$. *The vertical line indicates the rest frequency of the transition* $J_{Ka,Kc} = 27_{3,25} - 28_{0,28}$ *in the vibrationally excited* $SO_2(v_2=2)$ *bending mode of 345.01713 GHz*

| Hemisphere | Component | Temperature [K] | Mass [$M_\odot$] | Velocity Range [km $s^{-1}$] |
|---|---|---|---|---|
| **East** | **Infall** | 1000 ± 100 | (3.5 ± 1.2) x$10^{-5}$ | (-21 ± 3) to (-2 ± 1) |
| | **Outflow** | 1000 ± 100 | (1.9 ± 0.6) x$10^{-5}$ | (+3 ± 1) to (+20 ± 3) |
| **West** | **Infall** | 850 ± 50 | (7.0 ± 1.0) x$10^{-5}$ | (-13 ± 1) to (-2 ± 1) |
| | **Outflow** | 850 ± 50 | (5.0 ± 1.0) x$10^{-6}$ | (+13 ± 2) to (+20 ± 3) |

***Supplementary Table. 1.*** *Mass, average temperature, and velocity range for the molecular gas components that best match the observed spectra of the CO v=1, J=3-2 transition shown in Fig.3 without including a warm layer. The velocities indicate outflow (positive) and infall (negative) with respect to* $V_{*,lsr}$ *= 39.2 km* $s^{-1}$.